doi:10.1038/nature06325

ARTICLES

Crystal structure of the human β_2 adrenergic G-protein-coupled receptor

Søren G. F. Rasmussen[1]*, Hee-Jung Choi[1,2]*, Daniel M. Rosenbaum[1]*, Tong Sun Kobilka[1], Foon Sun Thian[1], Patricia C. Edwards[3], Manfred Burghammer[4], Venkata R. P. Ratnala[1], Ruslan Sanishvili[5], Robert F. Fischetti[5], Gebhard F. X. Schertler[3], William I. Weis[1,2] & Brian K. Kobilka[1]

Structural analysis of G-protein-coupled receptors (GPCRs) for hormones and neurotransmitters has been hindered by their low natural abundance, inherent structural flexibility, and instability in detergent solutions. Here we report a structure of the human β_2 adrenoceptor (β_2AR), which was crystallized in a lipid environment when bound to an inverse agonist and in complex with a Fab that binds to the third intracellular loop. Diffraction data were obtained by high-brilliance microcrystallography and the structure determined at 3.4 Å/3.7 Å resolution. The cytoplasmic ends of the β_2AR transmembrane segments and the connecting loops are well resolved, whereas the extracellular regions of the β_2AR are not seen. The β_2AR structure differs from rhodopsin in having weaker interactions between the cytoplasmic ends of transmembrane (TM)3 and TM6, involving the conserved E/DRY sequences. These differences may be responsible for the relatively high basal activity and structural instability of the β_2AR, and contribute to the challenges in obtaining diffraction-quality crystals of non-rhodopsin GPCRs.

GPCRs represent the largest family of membrane proteins in the human genome. They are remarkably versatile signalling molecules that are responsible for the majority of transmembrane signal transduction in response to hormones and neurotransmitters. GPCRs share a common structural signature of seven membrane-spanning helices with an extracellular N terminus and an intracellular C terminus (Fig. 1). Our understanding of GPCR structure has been based largely on the crystal structures of the inactive state of rhodopsin[1–7]. Rhodopsin is better suited for structural studies than most other GPCRs because it is possible to obtain large quantities of functional protein from bovine retina. Rhodopsin is also a remarkably stable GPCR, retaining function under conditions that denature other GPCRs.

The β_2AR is a GPCR activated by adrenaline that plays important parts in cardiovascular and pulmonary physiology, and is one of the most extensively characterized members of this large family of membrane proteins[8]. The sites of interactions between agonists and the receptor have been characterized by mutagenesis studies[9–12], and biophysical methods have been used to study the conformational changes associated with agonist binding and activation[13–18]. The β_2AR is efficiently expressed in Sf9 insect cells and can be purified to homogeneity using antibody and ligand affinity chromatography[19]. The β_2AR is biochemically pure following chromatography using an antibody resin that binds to an N-terminal Flag epitope; however, more than half of these purified receptor molecules are not functional. Affinity chromatography, an important early development in GPCR biochemistry[20], is essential for isolating functional β_2AR protein. Purified β_2AR bound to an antagonist remains stable and soluble at concentrations up to 50 mg ml^{-1} for up to a week at room temperature in the detergent dodecylmaltoside. However, the β_2AR is unstable in detergents used to obtain crystals of bovine rhodopsin. Extensive sparse matrix screening (over 2,000 conditions at 4 °C and 20 °C) failed to produce diffraction-quality crystals of wild-type β_2AR.

Challenges in crystallizing GPCRs

The difficulty in generating crystals from the wild-type β_2AR and other GPCRs for diffusible hormones and neurotransmitters may be related to the observation that these molecules are conformationally complex[18,21,22]. In contrast to rhodopsin, many GPCRs, including the β_2AR, exhibit significant basal, agonist-independent G protein activation. This basal activity has been associated with structural instability[23,24], suggesting that the intramolecular interactions that maintain the receptor in the inactive state are also important for the structural integrity of the protein. Orthosteric ligands for GPCRs exhibit a spectrum of efficacies for receptor-stimulated G protein activation, ranging from inverse agonists, which inhibit basal activity, to agonists, which maximally activate the receptor.

The β_2AR contains relatively unstructured regions that are involved in functionally important protein–protein interactions. Protease susceptibility and intramolecular fluorescence resonance energy transfer experiments[25] indicate that the C terminus and the third intracellular loop are the most unstructured regions. The N and C-terminal ends of the third intracellular loop are involved in G protein activation and the selectivity of GPCR–G protein interactions[26]. The C terminus interacts with G-protein-coupled receptor kinases, arrestins and other signalling molecules[27]. In the case of water-soluble proteins, removal of such unstructured regions can facilitate crystallization, but for the β_2AR this strategy would remove hydrophilic surfaces that are frequently observed to form lattice contacts in membrane-protein crystals.

Crystallization and structure solution

In an effort to provide conformational stability while increasing the polar surface available for crystal contacts, we generated a monoclonal antibody (Mab5) that binds to the third intracellular loop of native, but not denatured receptor protein[28]. Mab5 was generated

[1]Department of Molecular and Cellular Physiology and [2]Department of Structural Biology, Stanford University School of Medicine, 279 Campus Drive, Stanford, Palo Alto, California 94305, USA. [3]MRC Laboratory of Molecular Biology, Cambridge CB2 2QH, UK. [4]European Synchrotron Radiation Facility, 6 rue Jules Horowitz, BP220, 38043 Grenoble, cedex 9, France. [5]Biosciences Division, Argonne National Laboratory, GM/CA-CAT, Boulevard 436, D007, 9700 South Cass Avenue, Argonne, Illinois 60439, USA.
*These authors contributed equally to this work.

©2007 Nature Publishing Group

by immunizing mice with purified β_2AR reconstituted into phospholipid vesicles at a high protein-to-lipid ratio. Binding of Mab5 to β_2AR does not alter agonist or antagonist binding affinities, and does not prevent agonist-induced conformational changes[28]; therefore, it does not significantly alter the native structure of the receptor. Purified, deglycosylated β_2AR bound to carazolol (an inverse agonist) forms a complex with the Fab generated from Mab5 (Fab5) in detergent, and the β_2AR–Fab5 complex can be isolated by size-exclusion chromatography.

Crystals of the carazolol-bound β_2AR–Fab5 complex were grown in DMPC bicelles[29] using ammonium sulphate as a precipitant. The size and uniformity of the crystals were improved by removing 48 amino acids from the unstructured C terminus (β_2AR365, Fig. 1). Crystals of the β_2AR365–Fab5 complex grew as long, thin plates up to 300-μm long, approximately 30-μm wide, and less than 10-μm thick. Owing to the size and radiation sensitivity of the crystals, data collection required the use of microbeam technology[7,30] in which X-ray beams are either focused (ID-13 and ID23-2 beamlines, European Synchrotron Radiation Facility, Grenoble) or moderately focused and then further collimated (23ID-B GM/CA-CAT beamline, Advanced Photon Source) to diameters between 5 and 10 μm. The initial images from the best crystals showed diffraction to 3.0 Å; however, resolution was rapidly lost in sequential images from the same crystal volume. Nevertheless, we obtained a complete data set from a single crystal, and determined the structure by molecular replacement using immunoglobulin-domain search models for the Fab. The diffraction is anisotropic, with diffraction extending to 3.4 Å in the plane of the membrane and 3.7 Å perpendicular to the plane of the membrane.

Structure of the β_2AR–Fab5 complex

Figure 2a shows the packing of the β_2AR365–Fab5 complex in the crystals. The crystals seem to be formed from stacks of two-dimensional crystals, as previously reported for bacteriorhodopsin crystallized in bicelles[31]. There are few contacts between adjacent receptor molecules within a bicelle layer, indicating that the receptor is monomeric in the crystal. This is somewhat surprising considering that, in all reported crystals of rhodopsin, rhodopsin exists as antiparallel or parallel dimers[1–7]. Moreover, evidence from a variety of biochemical and biophysical studies suggest that the β_2AR and many other GPCRs exist as dimers or higher-order oligomers in the plasma membrane of cultured cells[32], and there may be a role for dimers in the export of properly folded receptor protein from the endoplasmic reticulum[32]. It is important to note, however, that β_2AR dimerization is not required for G protein activation. Purified β_2AR exists as monomers, and monomeric β_2AR reconstituted into recombinant high-density lipoprotein particles couples efficiently to G_s—its preferred heterotrimeric G protein[33].

The best-resolved regions of the crystal are the Fab5 fragments and cytoplasmic ends of the transmembrane segments of the receptor (Supplementary Fig. 1). In contrast to the cytoplasmic side of the receptor, the electron density is uninterpretable in the extracellular domain (Supplementary Fig. 2), even though this region of two receptor molecules packs together in a head-to-head manner around the crystallographic two-fold axis. The poor packing in this interface probably explains the significant anisotropy and poor overall resolution of the crystals. In an effort to improve the packing of the extracellular domains, we further modified β_2AR365 by inserting a TEV cleavage site after amino acid 24 (β_2AR24/365, Fig. 1). However, crystals of this construct are isomorphous to those made with β_2AR365, and the structure (Supplementary Table 1) is virtually identical to that obtained from β_2AR365–Fab5.

As expected, the overall structure of the β_2AR (Fig. 2b) is similar to rhodopsin, with seven transmembrane helices and an eighth helix that runs parallel to the cytoplasmic face of the membrane. Several of

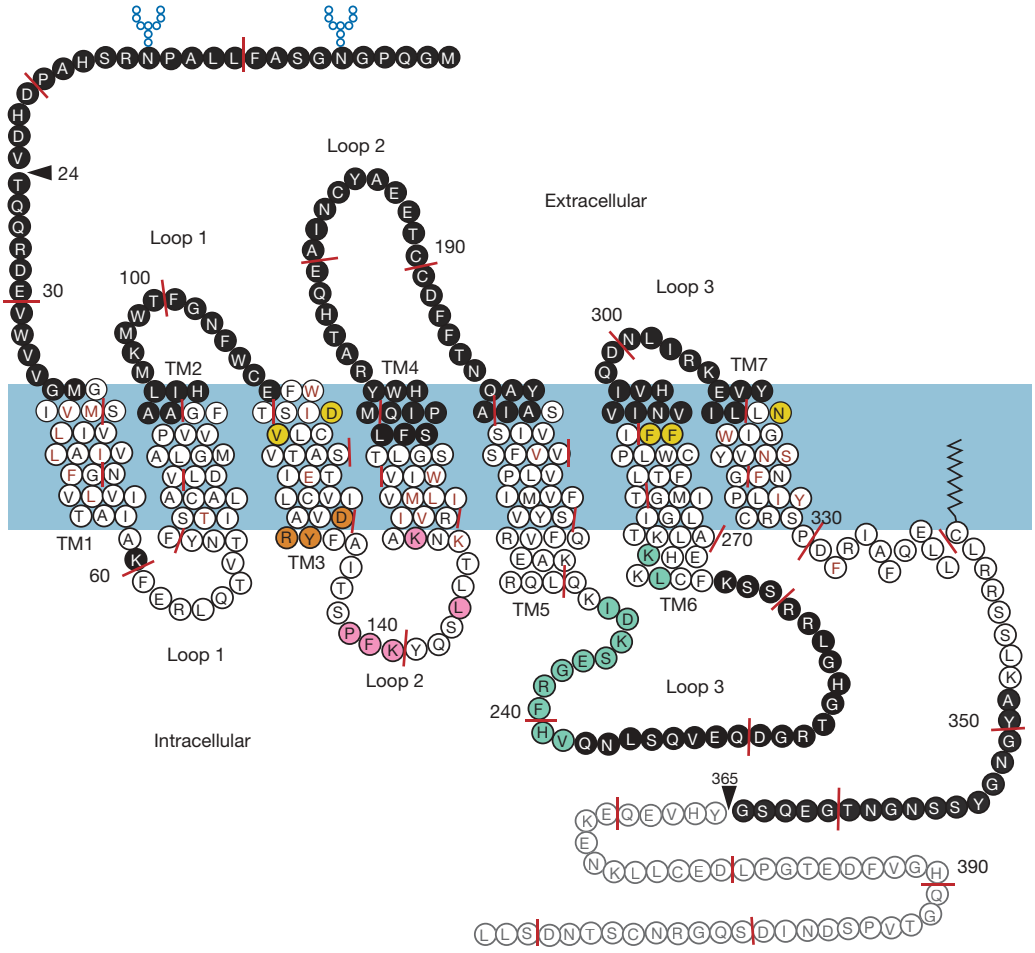

Figure 1 | Schematic diagram of the β_2AR. Black circles with white letters indicate disordered residues not included in the model. Grey letters and circles indicate residues not included in the β_2AR365 construct used for crystallography. Red letters indicate amino acids for which side-chain electron density was not modelled. Yellow residues indicate amino acids implicated in ligand binding from mutagenesis studies. Orange residues indicate the conserved DRY sequence. Green residues form the Fab5 epitope, and pink residues are packed against the Fab5 constant domain in the lattice. Small blue circles indicate glycosylation sites. Red lines indicate ten-amino-acid increments.

©2007 Nature Publishing Group

the transmembrane helices are broken by non-helical kinks, most prominently TM7. Residues not included in the β_2AR model, owing to absent or uninterpretable electron density, are indicated in Fig. 1. In the transmembrane helices, the majority of the missing side chains face the lipid environment. The loss of electron density occurs just above the ligand-binding site, near the predicted lipid-water interface, suggesting that ligand binding and/or the lipid environment contributes to the order of the transmembrane segments. Specific interactions between the variable domains of Fab5 and the β_2AR occur over a sequence of nine amino acids at the N-terminal end of intercellular loop 3 (I233–V242) and two amino acids at the C-terminal end (L266 and K270) (shown in green in Fig. 2b). Therefore, Fab5 recognizes a three-dimensional epitope on the β_2AR, which is in agreement with the observation that Fab5 binds to native, but not denatured β_2AR protein[28]. Additional lattice contacts occur between the constant domain of a symmetry-related Fab5 molecule and the second intracellular loop of β_2AR (shown in magenta in Fig. 2b).

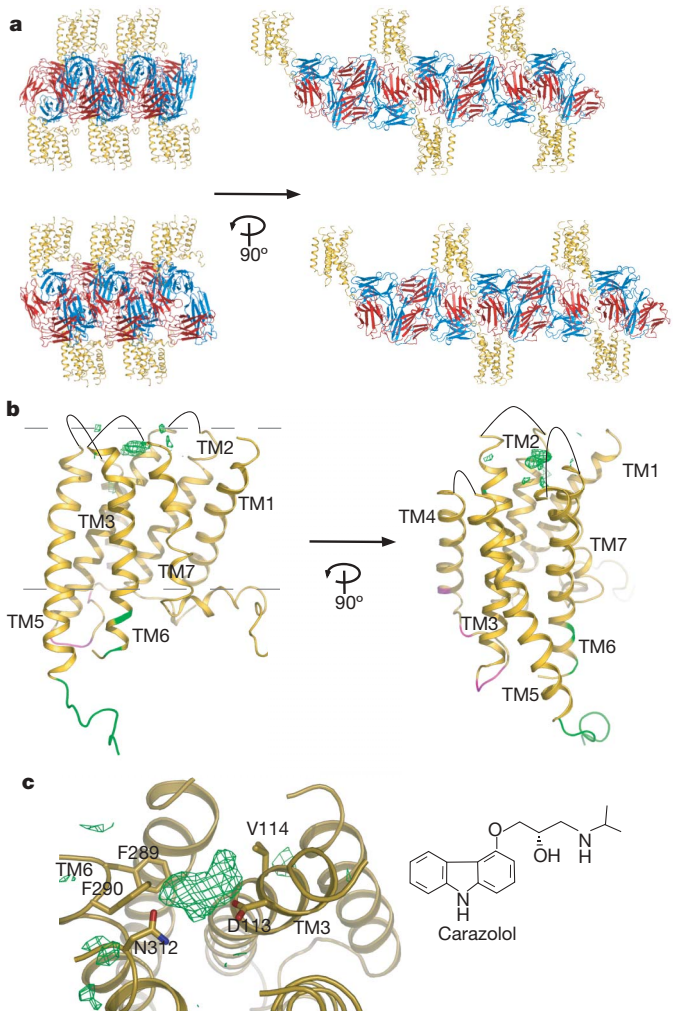

Figure 2 | Structure of the β_2AR365–Fab5 complex. **a**, Packing of the β_2AR365–Fab5 complex in crystals formed in DMPC bicelles (β_2AR, gold; heavy chain, blue; light chain, red). **b**, Structure of the β_2AR showing sites of the interactions with Fab5. Sites of specific (idiotypic) interactions between Fab5 and the β_2AR are shown in green. Sites of interactions between the β_2AR and the constant region of Fab5 of the symmetry mate are shown in magenta. Dotted grey lines indicate predicted membrane boundaries. Solid black lines indicate extracellular connections between transmembrane segments. **c**, F_O–F_C map contoured at 2.0 σ and surrounded by residues known to be involved in ligand binding. The chemical structure of carazolol, the bound ligand, is shown on the right.

Structural insights into basal activity

The ligand-binding site can be identified by an extended flat feature in the electron-density maps close to the extracellular side of the transmembrane helices (Fig. 2b, c). This is the only large feature in residual electron-density maps and is adjacent to Asp 113, Val 114, Phe 289, Phe 290 and Asn 312—residues identified from mutagenesis studies as being involved in ligand binding in the β_2AR[9,34,35]. This region corresponds to the retinal-binding site of rhodopsin. The weak electron density in this region precludes definitive modelling of carazolol. It is unlikely that the crystallization conditions resulted in dissociation of carazolol from β_2AR. Carazolol bound to the β_2AR has a distinct fluorescence emission spectrum[36], and β_2AR crystals and associated protein precipitate harvested from equilibrated hanging-drops showed no significant loss of carazolol binding, as detected by fluorescence spectroscopy (data not shown).

Figure 3 shows a comparison of transmembrane segments of the β_2AR superimposed with the homologous structure of rhodopsin. The root mean squared deviation for the alpha carbon backbone of the transmembrane segments is 1.56 Å. Although the overall arrangement of the transmembrane segments is similar, the β_2AR has a more open structure. The difference in the arrangement of the cytoplasmic ends of the transmembrane segments of β_2AR and rhodopsin may provide structural insights into basal receptor activity. Rhodopsin has no detectable basal activity, a feature essential for vision. In contrast, even when bound to the inverse agonist carazolol, the comparatively high basal activity of the β_2AR is suppressed by only 50% (Supplementary Fig. 4). Therefore, the carazolol bound β_2AR is not functionally equivalent to dark rhodopsin. Figure 3b compares the β_2AR and two rhodopsin structures at the level of the conserved (E/D)R(Y/W) sequence (found in 72% of rhodopsin family members)[18]. In the high-resolution structure of inactive (dark) rhodopsin, E134 and R135 in TM3 and E247 in TM6 form a network of hydrogen bonds and charge interactions referred to as the 'ionic lock'[37]. These interactions maintain rhodopsin in an inactive conformation. The ionic lock residues seem to have a similar role in the β_2AR because mutations of these amino acids in the β_2AR or other adrenergic receptors lead to constitutive activity[37,38]. Moreover, evidence from biophysical studies suggests that movement of the cytoplasmic end of TM3 relative to TM6 on activation is similar for the β_2AR and rhodopsin[17,39]. However, as shown in Fig. 3b, the transmembrane segments of the β_2AR have a more open structure in this region, and R131 in carazolol-bound β_2AR is not close enough to E268 to form a hydrogen bond. The structure of carazolol-bound β_2AR around the ionic lock is more similar to the structure of light-activated rhodopsin[40] (Fig. 3b), in which R135 and E247 are separated by 4.1 Å. This light-activated rhodopsin structure may not represent the fully active conformation because the spectral properties of these crystals are similar, but not identical, to those of metarhodopsin II[40]. Nevertheless, given the role of TM3, TM6 and the adjacent cytoplasmic loops in G protein coupling, the more open structure of the β_2AR may account for the residual basal activity of the β_2AR bound to the inverse agonist carazolol.

It is unlikely that the observed structural differences between the β_2AR and rhodopsin are due to distortion of the β_2AR owing to interactions between Fab5 and the third intracellular loop, because binding of Fab5 had no effect on agonist or antagonist binding affinity, and does not effect agonist-induced movement of TM3 relative to TM6 (ref. 28). However, we cannot exclude the possibility that crystal packing interactions between Fab5 and the second extracellular loop (Fig. 2b) contribute to these structural differences.

Another set of intramolecular interactions known to be important for minimizing the basal activity of the β_2AR involves L272 in TM6. Mutation of L272 to alanine was the first reported constitutively active mutant of the β_2AR[41]. As seen in Fig. 4, L272 forms extensive van der Waals interactions with I135 in TM3; V222 and Y219 in TM5; and Y141 in intracellular loop 2 (Fig. 4, and Supplementary Fig. 5). Because L272 is adjacent to E268, disruption of the packing interactions by mutation to alanine may have an effect similar to

©2007 Nature Publishing Group

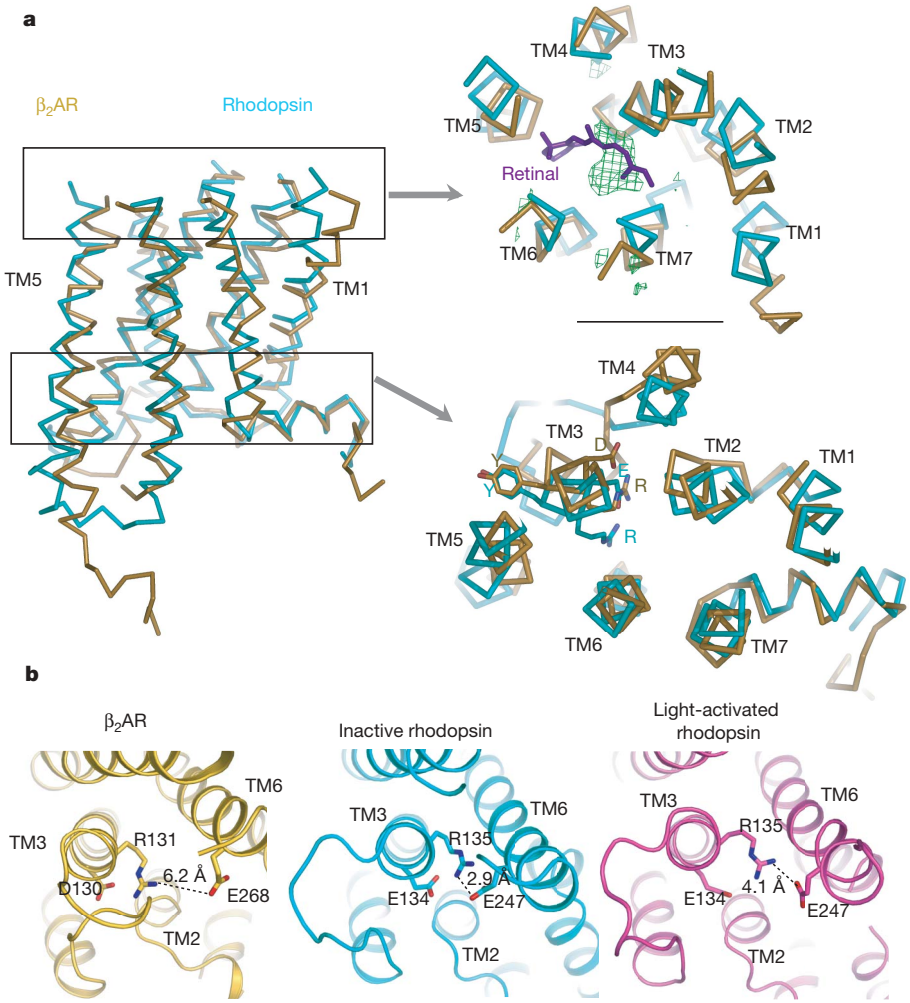

Figure 3 | Comparison of β_2AR and rhodopsin structures. **a**, The β_2AR is superimposed with the homologous structure of rhodopsin[6]. Retinal is shown in purple and the electron density in the putative ligand-binding site is shown as a green mesh. Structures were aligned using all seven transmembrane segments. The right panels represent cross-sections that are rotated 90° around the horizontal axis and viewed from the extracellular face of the receptor. **b**, Comparison of the β_2AR with structures of inactive rhodopsin and light-activated rhodopsin around the conserved E/DRY sequence in TM3. A dashed line shows the distance between the homologous arginine in TM3 and glutamate in TM6. To facilitate comparison of the E/DRY regions, the structures were aligned by superimposing TM3 only.

disruption of the ionic lock in rhodopsin. It is likely that this mutation would produce a more loosely packed, dynamic structure in this region, shifting the equilibrium towards a more active state.

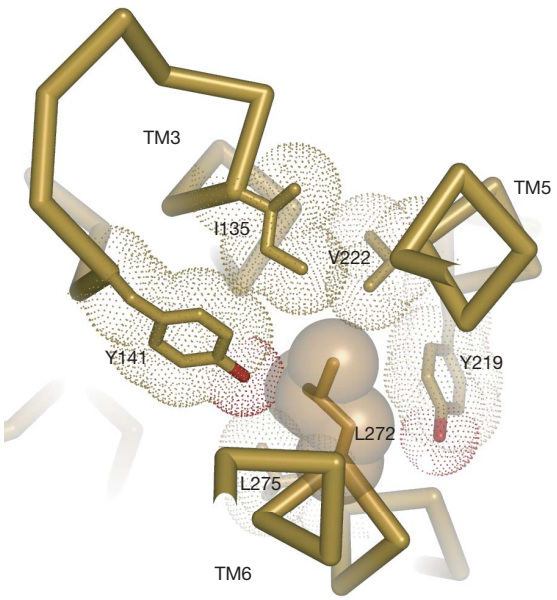

Figure 4 | Side-chain interactions between Leu 272 and residues in TM3, TM5 and intracellular loop 2. Packing interactions are reflected in lower *B*-factors for these amino acids. The average *B* value of residues 135, 141, 219, 222, 272 and 275 is 117 Å^2, compared to 157 Å^2 for the receptor as a whole.

It is interesting that packing interactions around L272 are observed while the ionic lock interactions are absent. Because mutation of either E268 or L272 leads to elevated basal activity, it is likely that both are involved in maintaining the basal state of the receptor. From the current structure, we can conclude that formation of the ionic lock and the tight packing of L272 are not interdependent, and might even be structurally incompatible. It is possible that the ionic lock and L272 interactions stabilize two of several distinct substates in the unliganded β_2AR, and that these two substates have lower activity towards G_s than the others. Carazolol binding may further stabilize the substate that favours packing around L272, and therefore reduce basal activity relative to the ensemble of substates in the unliganded receptor. The residual activity in the carazolol-bound receptor may be due to the failure to stabilize ionic lock interactions.

The limitations of this crystal structure of the β_2AR can be attributed to the poor crystal packing and the inherent structural flexibility of this GPCR relative to rhodopsin. Different crystallographic approaches will be needed to stabilize and visualize the extracellular domain and provide a more detailed picture of extracellular loops as well as the ligand-binding site. Nevertheless, this structure of the β_2AR in a lipid environment provides structural insights into the basis of basal activity, a feature of many GPCRs that may have both physiologic and therapeutic relevance.

METHODS SUMMARY

β_2AR was expressed in Sf9 insect cells using recombinant baculovirus. Sf9 cell membranes were solubilized in dodecylmaltoside and purified by sequential antibody and ligand affinity chromatography. Fab5 was generated by papain digestion of Mab5 and purified by ion-exchange chromatography. The β_2AR–Fab5 complex was formed by mixing purified β_2AR with a stoichiometric

©2007 Nature Publishing Group

excess of Fab5, and then isolated by size-exclusion chromatography. The purified β_2AR–Fab5 complex was mixed with bicelles composed of the lipid DMPC and the detergent CHAPSO. The final β_2AR–Fab concentration ranged between 8 and 12 mg ml^{-1}. Crystals were grown by hanging-drop vapour diffusion in a mixture of ammonium sulphate, sodium acetate and EDTA over a pH range of 6.5 to 7.5. Crystals grew within 7 to 10 days. They were cryoprotected in 20% glycerol before freezing in liquid nitrogen. Owing to the size and radiation sensitivity of the crystals, diffraction images were obtained by microcrystallography. The structure of the β_2AR365–Fab5 complex was solved by molecular replacement, using separate constant and variable Fab domain structures as search models. Coordinates and structure factors are deposited in the Protein Data Bank (accession codes 2R4R for β_2AR365–Fab5 and 2R4S for β_2AR24/365–Fab5).

Full Methods and any associated references are available in the online version of the paper at www.nature.com/nature.

Received 26 July; accepted 28 September 2007.
Published online 21 October 2007.

1. Okada, T. *et al.* X-Ray diffraction analysis of three-dimensional crystals of bovine rhodopsin obtained from mixed micelles. *J. Struct. Biol.* **130,** 73–80 (2000).
2. Palczewski, K. *et al.* Crystal structure of rhodopsin: A G protein-coupled receptor. *Science* **289,** 739–745 (2000).
3. Okada, T. *et al.* Functional role of internal water molecules in rhodopsin revealed by X-ray crystallography. *Proc. Natl Acad. Sci. USA* **99,** 5982–5987 (2002).
4. Teller, D. C., Okada, T., Behnke, C. A., Palczewski, K. & Stenkamp, R. E. Advances in determination of a high-resolution three-dimensional structure of rhodopsin, a model of G-protein-coupled receptors (GPCRs). *Biochemistry* **40,** 7761–7772 (2001).
5. Okada, T. *et al.* The retinal conformation and its environment in rhodopsin in light of a new 2.2 A crystal structure. *J. Mol. Biol.* **342,** 571–583 (2004).
6. Li, J., Edwards, P. C., Burghammer, M., Villa, C. & Schertler, G. F. Structure of bovine rhodopsin in a trigonal crystal form. *J. Mol. Biol.* **343,** 1409–1438 (2004).
7. Standfuss, J. *et al.* Crystal structure of a thermally stable rhodopsin mutant. *J. Mol. Biol.* **372,** 1179–1188 (2007).
8. Lefkowitz, R. J. The superfamily of heptahelical receptors. *Nature Cell Biol.* **2,** E133–E136 (2000).
9. Strader, C. D., Sigal, I. S. & Dixon, R. A. Structural basis of β-adrenergic receptor function. *FASEB J.* **3,** 1825–1832 (1989).
10. Wieland, K., Zuurmond, H. M., Krasel, C., Ijzerman, A. P. & Lohse, M. J. Involvement of Asn-293 in stereospecific agonist recognition and in activation of the β_2-adrenergic receptor. *Proc. Natl Acad. Sci. USA* **93,** 9276–9281 (1996).
11. Liapakis, G. *et al.* The forgotten serine. A critical role for Ser-203$^{5.42}$ in ligand binding to and activation of the β_2-adrenergic receptor. *J. Biol. Chem.* **275,** 37779–37788 (2000).
12. Strader, C. D., Candelore, M. R., Hill, W. S., Sigal, I. S. & Dixon, R. A. F. Identification of two serine residues involved in agonist activation of the β adrenergic receptor. *J. Biol. Chem.* **264,** 13572–13578 (1989).
13. Ghanouni, P., Steenhuis, J. J., Farrens, D. L. & Kobilka, B. K. Agonist-induced conformational changes in the G-protein-coupling domain of the β_2 adrenergic receptor. *Proc. Natl Acad. Sci. USA* **98,** 5997–6002 (2001).
14. Swaminath, G. *et al.* Sequential binding of agonists to the β_2 adrenoceptor: kinetic evidence for intermediate conformational states. *J. Biol. Chem.* **279,** 686–691 (2004).
15. Ghanouni, P. *et al.* Functionally different agonists induce distinct conformations in the G protein coupling domain of the β_2 adrenergic receptor. *J. Biol. Chem.* **276,** 24433–24436 (2001).
16. Swaminath, G. *et al.* Probing the β_2 adrenoceptor binding site with catechol reveals differences in binding and activation by agonists and partial agonists. *J.Biol. Chem.* **280,** 22165–22171 (2005).
17. Yao, X. *et al.* Coupling ligand structure to specific conformational switches in the β_2-adrenoceptor. *Nature Chem. Biol.* **2,** 417–422 (2006).
18. Kobilka, B. K. & Deupi, X. Conformational complexity of G-protein-coupled receptors. *Trends Pharmacol. Sci.* **28,** 397–406 (2007).
19. Kobilka, B. K. Amino and carboxyl terminal modifications to facilitate the production and purification of a G protein-coupled receptor. *Anal. Biochem.* **231,** 269–271 (1995).
20. Caron, M. G., Srinivasan, Y., Pitha, J., Kociolek, K. & Lefkowitz, R. J. Affinity chromatography of the β-adrenergic receptor. *J. Biol. Chem.* **254,** 2923–2927 (1979).
21. Kenakin, T. Ligand-selective receptor conformations revisited: the promise and the problem. *Trends Pharmacol. Sci.* **24,** 346–354 (2003).
22. Kobilka, B. K. G protein coupled receptor structure and activation. *Biochim. Biophys. Acta* **1768,** 794–807 (2006).
23. Gether, U. *et al.* Structural instability of a constitutively active G protein-coupled receptor. Agonist-independent activation due to conformational flexibility. *J. Biol. Chem.* **272,** 2587–2590 (1997).
24. Samama, P., Bond, R. A., Rockman, H. A., Milano, C. A. & Lefkowitz, R. J. Ligand-induced overexpression of a constitutively active β_2-adrenergic receptor: Pharmacological creation of a phenotype in transgenic mice. *Proc. Natl Acad. Sci. USA* **94,** 137–141 (1997).
25. Granier, S. *et al.* Structure and conformational changes in the C-terminal domain of the β_2-adrenoceptor: insights from fluorescence resonance energy transfer studies. *J. Biol. Chem.* **282,** 13895–13905 (2007).
26. Gether, U. & Kobilka, B. K. G protein-coupled receptors. II. Mechanism of agonist activation. *J. Biol. Chem.* **273,** 17979–17982 (1998).
27. Reiter, E. & Lefkowitz, R. J. GRKs and β-arrestins: roles in receptor silencing, trafficking and signaling. *Trends Endocrinol. Metab.* **17,** 159–165 (2006).
28. Day, P. W. *et al.* A monoclonal antibody for G protein coupled receptor crystallography. *Nature Methods* doi:10.1038/nmeth1112 (21 October2007).
29. Faham, S. *et al.* Crystallization of bacteriorhodopsin from bicelle formulations at room temperature. *Protein Sci.* **14,** 836–840 (2005).
30. Riekel, C., Burghammer, M. & Schertler, G. Protein crystallography microdiffraction. *Curr. Opin. Struct. Biol.* **15,** 556–562 (2005).
31. Faham, S. & Bowie, J. U. Bicelle crystallization: a new method for crystallizing membrane proteins yields a monomeric bacteriorhodopsin structure. *J. Mol. Biol.* **316,** 1–6 (2002).
32. Bulenger, S., Marullo, S. & Bouvier, M. Emerging role of homo- and heterodimerization in G-protein-coupled receptor biosynthesis and maturation. *Trends Pharmacol. Sci.* **26,** 131–137 (2005).
33. Whorton, M. R. *et al.* A monomeric G protein-coupled receptor isolated in a high-density lipoprotein particle efficiently activates its G protein. *Proc. Natl Acad. Sci. USA* **104,** 7682–7687 (2007).
34. Suryanarayana, S., Daunt, D. A., Von Zastrow, M. & Kobilka, B. K. A point mutation in the seventh hydrophobic domain of the α_2 adrenergic receptor increases its affinity for a family of β receptor antagonists. *J. Biol. Chem.* **266,** 15488–15492 (1991).
35. Chelikani, P., Hornak, V., Eilers, M., Reeves, P. J., Smith, S. O., RajBhandary, U. L. & Khorana, H. G. Role of group-conserved residues in the helical core of β_2-adrenergic receptor. *Proc. Natl Acad. Sci. USA* **104,** 7027–7032 (2007).
36. Tota, M. R. & Strader, C. D. Characterization of the binding domain of the β-adrenergic receptor with the fluorescent antagonist carazolol. Evidence for a buried ligand binding site. *J. Biol. Chem.* **265,** 16891–16897 (1990).
37. Ballesteros, J. A. *et al.* Activation of the β_2-adrenergic receptor involves disruption of an ionic lock between the cytoplasmic ends of transmembrane segments 3 and 6. *J. Biol. Chem.* **276,** 29171–29177 (2001).
38. Scheer, A. *et al.* Mutational analysis of the highly conserved arginine within the Glu/Asp-Arg-Tyr motif of the α_{1b}-adrenergic receptor: effects on receptor isomerization and activation. *Mol. Pharmacol.* **57,** 219–231 (2000).
39. Farrens, D. L., Altenbach, C., Yang, K., Hubbell, W. L. & Khorana, H. G. Requirement of rigid-body motion of transmembrane helices for light activation of rhodopsin. *Science* **274,** 768–770 (1996).
40. Salom, D. *et al.* Crystal structure of a photoactivated deprotonated intermediate of rhodopsin. *Proc. Natl Acad. Sci. USA* **103,** 16123–16128 (2006).
41. Samama, P., Cotecchia, S., Costa, T. & Lefkowitz, R. J. A mutation-induced activated state of the β_2-adrenergic receptor. Extending the ternary complex model. *J. Biol. Chem.* **268,** 4625–4636 (1993).

Supplementary Information is linked to the online version of the paper at www.nature.com/nature.

Acknowledgements This study was supported by the Lundbeck Foundation (S.G.F.R.), a National Institutes of Health Ruth L. Kirchstein NRSA grant (D.M.R.), a National Institute of General Medical Sciences grant (W.I.W.), a National Institute of Neurological Disorders and Stroke grant, the Mather Charitable Foundation, and a generous gift from Lundbeck (to B.K.K). G.F.X.S. was financially supported by a Human Frontier Science Project (HFSP) programme grant, a European Commission FP6 specific targeted research project and an ESRF long-term proposal. We thank R. Mackinnon and J. Bowie for advice, R. Stevens for help with early screening efforts, and J. Smith for arranging access to GM/CA-CAT at the APS. Use of the APS is supported by the US Department of Energy. GM/CA-CAT is funded by the US National Institutes of Cancer and General Medical Sciences. We thank X. Deupi and S. Granier for help with data collection. We thank D. Flot for his support at the ID 23.2 microfocus beamline at the European Synchrotron Radiation Facility.

Author Contributions S.G.F.R. performed final stages of β_2AR purification, purified Mab5 and prepared Fab5. D.M.R. generated recombinant β_2AR used for crystallography. Crystal screening and optimization were performed by S.G.F.R. and D.M.R. H.J.C. assisted with data collection at the Advanced Photon Source, processed all diffraction data and solved the structure of the β_2AR–Fab5 complex. F.S.T. expressed β_2AR in insect cells and, together with T.S.K., performed the initial stage of β_2AR purification. T.S.K. prepared antibody 5. W.I.W. supervised and assisted with data collection at the Advanced Photon Source, and with data processing and structure determination. G.F.X.S. introduced B.K.K. to microfocus diffraction technology and supervised data collection at the European Synchrotron Radiation Facility. P.C.E. and M.B. assisted with data collection at the European Synchrotron Radiation Facility. R.S. and R.F.F. assisted with data collection at the Advanced Photon Source. V.R.P.R. performed the functional characterization of carazolol. B.K.K .was responsible for the overall project management and strategy, and assisted with β_2AR purification, crystal harvesting and synchrotron data collection. B.K.K., W.I.W. and G.F.X.S. prepared the manuscript. All authors discussed the results and commented on the manuscript.

Author Information Reprints and permissions information is available at www.nature.com/reprints. Correspondence and requests for materials should be addressed to B.K.K. (kobilka@stanford.edu).

©2007 **Nature Publishing Group**

METHODS

Crystallization. Preparation of β_2AR365 and Fab5 are described in Supplementary Methods. The β_2AR365–Fab5 complexes were mixed with bicelles (10% w/v 3:1 DMPC:CHAPSO in 10 mM HEPES, pH 7.5, 100 mM NaCl) at a 1:5 (protein:bicelle) ratio, and crystals were grown in sitting- and hanging-drop formats at 22 °C using equal volumes of protein mixture and reservoir solutions. Initial crystallization leads were identified using multiple 96-well sitting-drop screens from Nextal (Qiagen). After extensive optimization, crystals for data collection were grown in hanging-drop format over a reservoir solution of 1.85–2.0 M ammonium sulphate, 180 mM sodium acetate, 5 mM EDTA, 100 mM MES or HEPES, pH 6.5–7.5. Crystals grew to full size within 7 to 10 days. Crystals were flash frozen and stored in liquid nitrogen, with reservoir solution plus 20% glycerol as cryoprotectant.

Microcrystallography data collection and processing. Microbeams were essential to obtain a favourable signal-to-noise ratio from the weakly diffracting thin crystals. The shape of the crystals permitted complete data to be measured from a single crystal. A small wedge of data, typically 5–10°, (1° per frame) could be measured before significant radiation damage was observed. The crystal was then translated to a new, undamaged position to collect the next wedge of data. A total of 182° of data collected in this manner, measured at beamline ID23-2 of the ESRF, were used for the final β_2AR365–Fab5 data set (Supplementary Table 1). The β_2AR24/365–Fab5 data set was obtained from 225° of data measured using a 4-μm × 6-μm beam at beamline 23ID-B of the APS (Supplementary Table 1).

ESRF data were processed with MOSFLM and SCALA[42], and data measured at the APS were processed with HKL2000[43]. In many cases it was necessary to re-index the crystal after moving to a new position on the crystal, which may have been due to bending of the frozen crystals such that the indexing matrix from the previous volume could not accurately predict the diffraction pattern from a new volume. This problem precluded global post refinement of the unit cell parameters. The unit cell parameters used for subsequent analysis (Supplementary Table 1) were obtained from initial indexing and refinement from one wedge of the ESRF data, and were subsequently found to be sufficient for processing the remaining data without unit cell constant refinement. Using a partial specific volume of 1.21 Å^3/Da for protein, the unit cell would have 66% lipid, detergent and aqueous solvent for one β_2AR–Fab5 complex in the asymmetric unit.

Structure solution and refinement. The structure of the β_2AR365–Fab5 complex was solved by molecular replacement, by searching with separate constant and variable domain models against a low-resolution (4.1 Å) data set measured at ESRF beamline ID-13. The Fab was derived from a murine IgG antibody containing a κ light chain and γ1 heavy chain[28]. At the time of these calculations the sequence of the heavy chain was not known, and the crystal structure of a Fab containing a κ light chain but γ2 heavy chain[44] (PDB code 1IGT) was used as a search model. Molecular replacement was performed with the program PHASER[45], using data between 12 and 4.5 Å. The constant domain was placed first, followed by the variable domain. The constant domain model retained all side chains, whereas the variable domain was reduced to polyalanine. All atomic temperature factors were set to 50 Å^2. The best solution had rotation and translation function Z scores of 5.3 and 10.6 for the constant domain, and 4.5 and 21.7 for the variable domain. An electron density map calculated to 6 Å from this solution revealed rods of density corresponding to the transmembrane helices of the receptor. A model of the transmembrane portion of rhodopsin made by removing the cytoplasmic and extracellular loops, retinal and water molecules, and replacing those residues non-identical with β_2AR with alanine could be manually placed into this density. To obtain a convenient starting model for building the receptor, the molecular replacement calculation was re-run to include the rhodopsin transmembrane helices model as a third search model after placing the two Fab domains. Although the top solution was not very strong statistically (rotation function $Z = 2.5$, translation function $Z = 7.0$), after rigid body refinement the rhodopsin model was very close to that placed manually into the 6 Å map. This molecular replacement solution was then subjected to rigid-body refinement between 20 and 5 Å in CNS[46], using five rigid bodies (the Fab constant domain light and heavy chains, the variable domain light and heavy chains, and rhodopsin). This gave R and R_{free} values of 0.447 and 0.452, respectively.

Electron-density maps made with phases either from the Fab model alone or the rigid-body refined Fab + minimal rhodopsin model indicated significant differences between rhodopsin and β_2AR, and extensive manual rebuilding was required to refine the structure. The structure was initially refined at 4.1 Å resolution. The test set from the 4.1 Å set was transferred to the higher-resolution β_2AR365–Fab5 set measured at the ESRF (Supplemental Table 1) and additional test set reflections added in the 4.1–3.4 Å range. Multiple rounds of manual rebuilding, positional and grouped temperature factor refinement were performed using the maximum likelihood amplitude target in CNS. The electron density of the Fab is very well defined owing to its tight packing in the crystal, whereas the receptor is poorly packed and has much higher temperature factors (Supplementary Fig. 1 and Supplementary Table 1). Because the receptor density is poor, we also refined against a second data set from a single crystal of the β_2AR24/365–Fab5 complex (Supplementary Table 1), to ensure that any densities observed in the receptor region are not due to noise in the first data set. The β_2AR24/365–Fab5 data set was obtained from 225° of data measured using a 4-μm × 6-μm beam at beamline 23ID-B of the APS. Although there is electron density in the extracellular region, the final model retains only those residues that could be unambiguously assigned (Fig. 1).

The high-temperature factors and weak electron density for the receptor raises concerns about model bias. However, the Fab represents 50% of the scattering mass and, because of its better order, contributes even more to the total scattering and so represents a significant source of phase information independent of the receptor. Simulated annealing omit maps confirmed the interpretation presented here. Moreover, alternative sequence registers or backbone paths were considered in several portions of the receptor, but these models could be eliminated based on inspection of σ_A weighted $2F_O–F_C$ and $F_O–F_C$ electron density maps.

On the basis of the average $F/\sigma(F)$ of reflections near the three crystallographic axes (as defined by the program TRUNCATE[32]), we estimate the effective resolution to be 3.4 Å within the plane of the membrane and 3.7 Å perpendicular to the membrane for the β_2AR365–Fab5 structure, and 3.4 Å/3.8 Å for the β_2AR24/365–Fab5 structure.

42. Collaborative Computational Project. N. The CCP4 suite: programs for protein crystallography. *Acta Crystallogr. D* **50**, 760–763 (1994).
43. Otwinowski, Z. & Minor, W. Processing of x-ray diffraction data collected in oscillation mode. *Methods Enzymol.* **276**, 307–326 (1997).
44. Harris, L. J., Larson, S. B., Hasel, K. W. & McPherson, A. Refined structure of an intact IgG2a monoclonal antibody. *Biochemistry* **36**, 1581–1597 (1997).
45. McCoy, A. J. Solving structures of protein complexes by molecular replacement with Phaser. *Acta Crystallogr. D* **63**, 32–41 (2007).
46. Brünger, A. T. *et al.* Crystallography and NMR System (CNS): A new software system for macromolecular structure determination. *Acta Crystallogr. D* **54**, 905–921 (1998).

©2007 Nature Publishing Group